# A Battery-Less Backscatter Tag Supporting Energy- and Spectrally-Efficient Bidirectional WiFi Communication and Ad Hoc Networking

Yongliang Zhang, Ji Xiong, Tianle Tang, Wenjun Zhao, Jiangfeng Wu, and Miao Meng

School of Electronics and Information Engineering, Tongji University, Shanghai, China

Email: miaomeng@tongji.edu.cn

***Abstract*—This paper presents the first backscatter tag that supports both bidirectional WiFi communication and ad hoc networking, enabled by proposing a reconfigurable inductor-less, fully-integrated SSB B/QPSK pulse-shaped backscatter transmitter (TX) and a passive heterodyne DBPSK receiver (RX). When implemented with commodity WiFi TRXs, the tag achieves the best-reported single antenna communication range of 36m in the worst case and power consumption of 4.3μW for downlink and 6.6μW for uplink, respectively, allowing battery-less operation when harvesting from BLE energy.**

***Keywords—backscatter, WiFi, low-power, energy-efficient.***

## I. Introduction

WiFi is the most ubiquitous wireless network technology for IoTs in residential, workplace, and commercial environments. However, the power consumption of conventional WiFi transceivers (10s to 100s of mW) is prohibitively high for emerging IoT devices. Recent work in WiFi backscattering has demonstrated ultra-low power connectivity (<50μW) while maintaining compatibility with existing infrastructure [1]-[7]. To enable pragmatic adoption at a large scale with limited spectral resources, despite ultra-low power, such WiFi backscatter tags should ideally support 1) bidirectional WiFi communication and 2) peer-to-peer, ad hoc communication. Unfortunately, a low-power backscatter IC that can simultaneously achieve the above specifications has not been demonstrated (Fig.1a). For example, prior work only supports unidirectional WiFi communication: [1]-[6] achieve WiFi-compatible uplink, but the energy-detecting OOK downlink receiver (RX) only wakes up the tag at a rate of < 65kbps, demodulation of the WiFi packets directly from commercial devices is not possible. [7] equips a rectifier-based WiFi 802.11b-DBPSK demodulator; however, the adopted GFSK uplink is not supported by WiFi and thus the system requires an additional BLE RX. It is also worth mentioning that existing backscattering tags are limited to communicating on a few selected WiFi channels (1 in [4], [5] and [7], 2 in [1]-[3], 8 in [6]), which can potentially exacerbate communication latency in crowded networks. And most importantly, no WiFi tag yet supports peer-to-peer communication.

This paper presents the first battery-less backscatter IC featuring bidirectional WiFi communication and peer-to-peer, ad hoc networking (Fig. 1b) by: 1) unlocking a new passive heterodyne DBPSK RX to allow a fully WiFi compatible downlink communication; 2) proposing an inductor-less reconfigurable SSB Q/BPSK backscatter TX; 3) introducing a pulse-shaping B/QPSK backscatter technique to enable spectral efficient peer-to-peer communication; 4) employing an ultra-low-voltage-wide-band phase lock loop (ULVWBPLL) with automatic frequency control (AFC) to support frequency-translation from three BLE advertisement channels (CH.37-39) to all 802.11b channels at ultra-low power (64 cases in total); 5) integrating a RF energy harvester (EH), permitting efficient BLE energy harvesting with improved range.

This work was supported in part by NSFC 62174120.

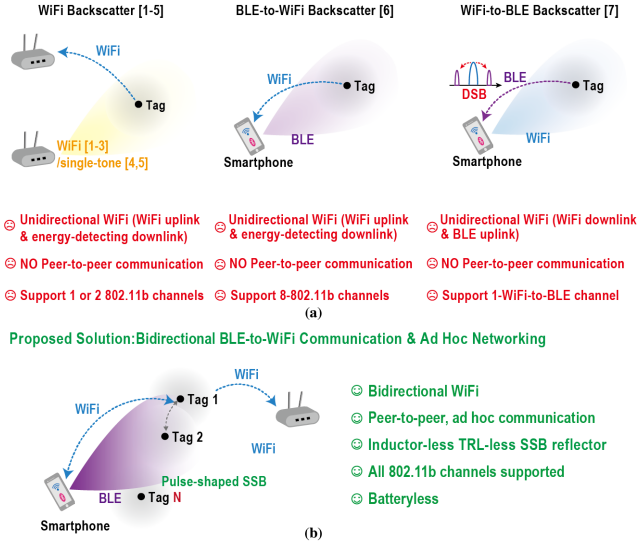


Fig. 1. (a) Overview of prior WiFi backscatter approaches; (b) key features of the proposed backscatter chip.

## II. System Architecture and Implementation

### A. System Overview

Fig. 2 depicts the block diagram of the proposed backscatter IC. A 6-stage self-compensated rectifier [8] and a power management unit (PMU) are used to harvest incident BLE energy and establish the power source and references for the whole chip. Then, a 22MHz crystal oscillator (XTAL) starts up, and the proposed passive heterodyne RX is activated when XTAL is stabilized. The AFC-assisted ULVWBPLL is turned on upon uplink request, while the demodulator is turned off to conserve energy. The AFC calibrates the VCO frequencies according to the frequency translation needs; it leverages the quadrature phase of VCO to expedite the calibration, achieving a total locking time of less than 20μs with high precision. Finally, backscattering is achieved via the proposed reconfigurable TX. The frequency generation block implementing the AFC-assisted ULVWBPLL is shown in Fig. 3a. It utilizes a 250kHz clock (divided from the 22MHz XTAL) as the reference, generating an IF ranging from 12.75MHz to 70.25MHz, thus supporting frequency translation from all three BLE

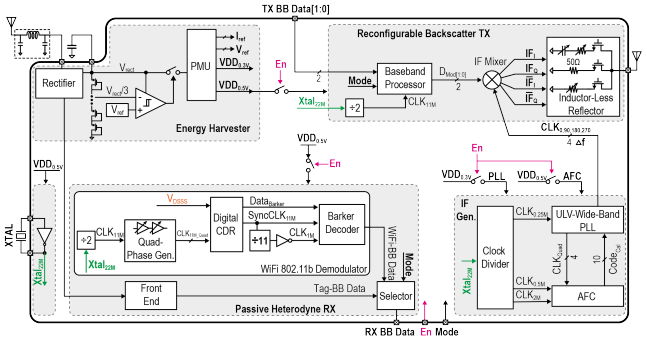


Fig. 2. The block diagram of the proposed backscatter tag includes an energy harvester, an IF generation block, the proposed passive heterodyne RX block, and the proposed reconfigurable backscatter transmitter block.

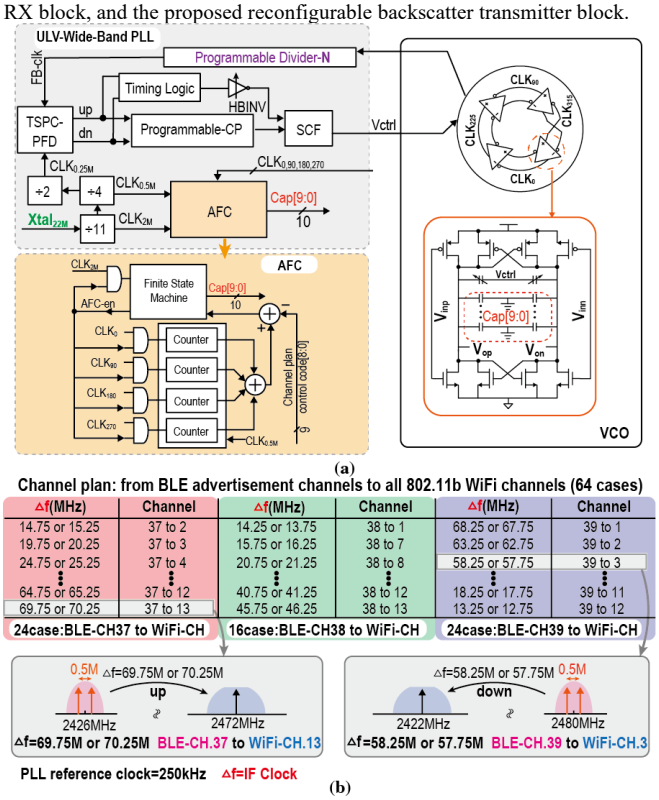


| Δf(MHz) | Channel | Δf(MHz) | Channel | Δf(MHz) | Channel |
|---|---|---|---|---|---|
| 14.75 or 15.25 | 37 to 2 | 14.25 or 13.75 | 38 to 1 | 68.25 or 67.75 | 39 to 1 |
| 19.75 or 20.25 | 37 to 3 | 15.75 or 16.25 | 38 to 7 | 63.25 or 62.75 | 39 to 2 |
| 24.75 or 25.25 | 37 to 4 | 20.75 or 21.25 | 38 to 8 | 58.25 or 57.75 | 39 to 3 |
| ⋮ | ⋮ | ⋮ | ⋮ | ⋮ | ⋮ |
| 64.75 or 65.25 | 37 to 12 | 40.75 or 41.25 | 38 to 12 | 18.25 or 17.75 | 39 to 11 |
| 69.75 or 70.25 | 37 to 13 | 45.75 or 46.25 | 38 to 13 | 13.25 or 12.75 | 39 to 12 |

Fig. 3. (a) the frequency generation block implementing the proposed AFC assisted-ULVWBPLL; (b) the channel plan translating three BLE advertisement channels to all 802.11b WiFi channels.

advertisement channels to every 802.11b WiFi channel (64 cases), as illustrated in Fig. 3b. With a 0.3V supply, it achieves a measured phase noise of -107dBc/Hz at 1MHz offset and a measured reference spur level of -50.4dBc, which are well compiled with the requirement for 802.11b modulation, all with a minimum of 3.2μW power consumption.

## B. The Proposed Passive Heterodyne Receiver

Fig. 4 illustrates the proposed passive heterodyne receiver. During Smartphone/access point (AP)-to-tag downlink, simultaneous BLE tone and 802.11b WiFi packet are incident on the RX antenna, inspired by [9], the frequency down-conversion ($\Delta f = f_{BLE} - f_{WiFi}$) is achieved passively by leveraging the non-linearity of energy harvester (EH). The demodulator leverages the fact that the phase-flipping (PF) information is encoded in the envelope of the DBPSK-modulated 802.11b WiFi packet (PF happens when the envelope is at its minimum). Therefore, by amplifying the down-converted signal into pulses, wider pulses can be

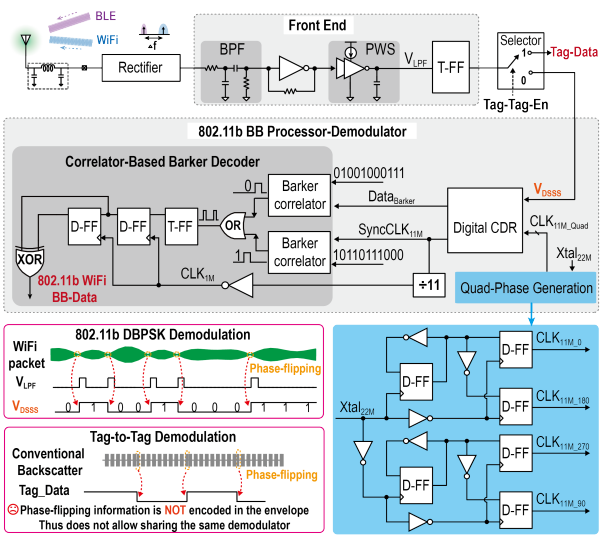


Fig. 4. Concept and circuit implementation of the proposed passive heterodyne receiver.

recovered at every PF point. Then a two-stage pulse-width-shrinker (PWS) is implemented to remove the pulses with narrower widths, followed by a T-flip-flop (T-FF) to recover the 11Mbps DSSS data ($V_{DSSS}$, 1Mbps WiFi-baseband data multiplied by 11Mbps Barker code). $V_{DSSS}$ is then fed into the proposed Barker decoder containing two 11b-digital-Barker-correlators with soft-decision decoding to enable low-power and robust WiFi-baseband (BB) data recovery. In the ad hoc mode, the Barker demodulator can be disabled and bypassed for a faster peer-to-peer data rate; however, unlike the 802.11b DBPSK signal, the envelope of conventional backscattered DBPSK signals does not carry PF information, making low-power demodulation impossible. Therefore, a reconfigurable SSB pulse-shaping backscatter TX is proposed to create WiFi-like backscattered signals.

## C. Proposed Reconfigurable Backscatter Transmitter

The concept and implementation of the proposed transmitter are shown in Fig. 5. The key idea of the proposed pulse-shaping modulator is to provide a smooth envelope transition at data symbol boundaries and let the phase change when the envelope is at its minimum (similar to WiFi). Cycling through a single SP3T switch with three non-overlapping 90°-delayed switching signals ($S_{1\text{-}3}$) generated by IF, SSB frequency translating I and Q reflective paths are created, where the I-reflective path connects to resistive loads ($\Gamma_{Res} = |\Gamma_{Res}|e^{j0°}$), and the Q-reflective path connects to the corresponding capacitive loads ($\Gamma_{Cap} = |\Gamma_{Cap}|e^{-j90°}$). At data symbol boundaries, $|\Gamma_{Res}|$ and $|\Gamma_{Cap}|$ first decrease linearly in pair ($\Gamma_0$ to $\Gamma_4$) until they reach the minimum (this can be done by a pair of 5-1 selectors controlled by $\Gamma[2:0]$), then the phase-change is triggered by changing the leading/lagging condition of the quadrature clock generating the IF. When the phase change is completed, $|\Gamma_{Res}|$ and $|\Gamma_{Cap}|$ then change in the reversed order ($\Gamma_4$ to $\Gamma_0$) to their maximum. As a result, SSB pulse-shaped Q/BPSK modulation can be realized to create a WiFi-like backscatter signal. In addition, by eliminating the abrupt phase transitions at symbol boundaries, sidelobe suppression is also achieved to further improve the spectrum efficiency, allowing data rate enhancement and potential spectrally efficient concurrent-multi-pair peer-to-peer communication within the limited bandwidths. It should be noted that, during Tag-to-Smartphone/AP communication,

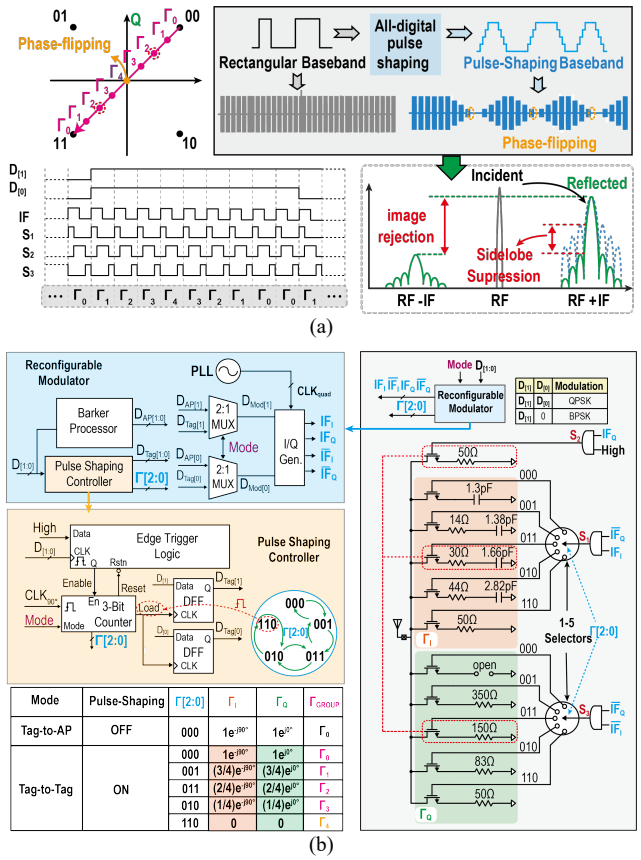


| Mode | Pulse-Shaping | Γ[2:0] | $\Gamma_I$ | $\Gamma_Q$ | $\Gamma_{GROUP}$ |
|---|---|---|---|---|---|
| Tag-to-AP | OFF | 000 | $1e^{j90°}$ | $1e^{0°}$ | $\Gamma_0$ |
| Tag-to-Tag | ON | 000 | $1e^{j90°}$ | $1e^{0°}$ | $\Gamma_0$ |
| | | 001 | $(3/4)e^{j90°}$ | $(3/4)e^{0°}$ | $\Gamma_1$ |
| | | 011 | $(2/4)e^{j90°}$ | $(2/4)e^{0°}$ | $\Gamma_2$ |
| | | 010 | $(1/4)e^{j90°}$ | $(1/4)e^{0°}$ | $\Gamma_3$ |
| | | 110 | 0 | 0 | $\Gamma_4$ |

Fig. 5. (a) concept of the proposed reconfigurable pulse-shaped backscatter transmitter; (b) circuits implementation.

where the pulse-shaping is not necessary, the proposed structure can be reconfigured to connect $S_{1\text{-}3}$ to capacitive ($\Gamma_0=e^{-j90°}$), absorbing ($\Gamma=0$), and open ($\Gamma_{Res}=e^{j0°}$), respectively, allowing to backscatter with only two switches (the open reflection condition does not require a switch), without the requirement of any off-chip component, achieving a tuning-free SSB Q/BPSK backscattering with the best-reported area efficiency.

## III. Measurement Results

The backscatter IC was fabricated in 65nm CMOS, occupying a core area of 0.33mm$^2$. Fig. 6 demonstrates that the chip can successfully harvest BLE energy on a 1µF storage capacitor, start the 1µW crystal oscillator and the 3.3µW DBPSK demodulator in sequence, and turn on the reconfigurable transmitter upon request.

Fig. 7 shows the measured demodulation waveforms with input power at -17dBm for the two cases: 1) AP/smartphone-to-Tag: WiFi 802.11b data on WiFi-CH.4 is demodulated utilizing a BLE tone on BLE-CH.39; 2) Tag-to-Tag: demodulation at 5Mbps data rate with an offset frequency of 41.25 MHz, utilizing a BLE tone on BLE-CH.38.

Fig. 8 demonstrates the generation of frequency-translated packets to every 802.11b WiFi channel (WiFi-CH. 1-13) implementing the AFC-assisted ULVWBPLL. Thanks to the inductor-less reflector, the SSB modulator achieves the best-reported image rejection of 33dB (20dB improvement over [3]). Moreover, the proposed pulse-shaping technique suppresses the first sidelobe by 12dB compared to the same modulator without pulse-shaping.

Fig. 9 shows that the chip can achieve stable EVM performance across various IFs (with a symbol rate of

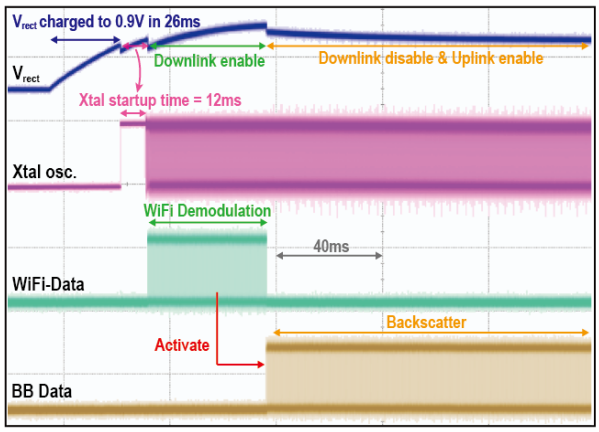


Fig. 6. Measured system workflow.

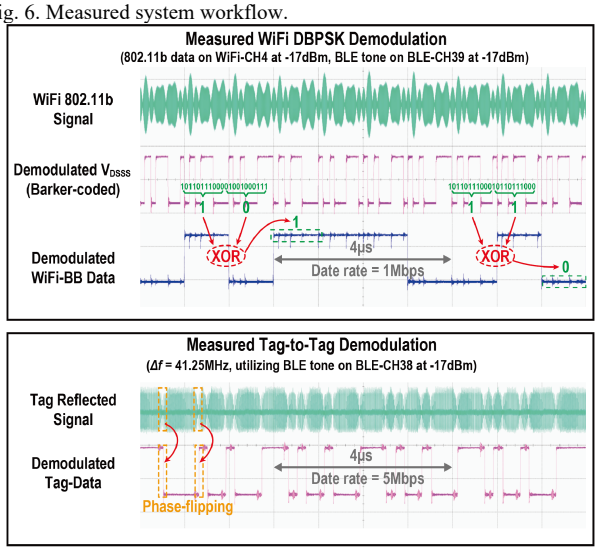


Fig.7. Measured WiFi 802.11b DBPSK and Tag-to-Tag demodulation waveforms.

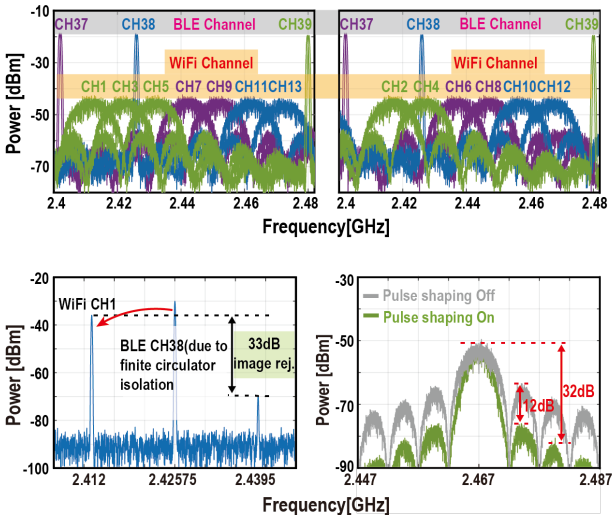


Fig. 8. Measured spectra showing SSB frequency translation from BLE to all WiFi channels (top); SSB performance (bottom left); and effectiveness of pulse-shaping (bottom right).

1Msps). During backscattering, the chip consumes an active power of 6.6µW at an IF of 15.25MHz (BLE-CH. 37 to WiFi-CH. 2) and less than 16µW across all channels (power varies corresponding to different IF frequencies).

Wireless experiments with commercial TRX hardware are shown in Fig. 10. The chip can be powered up within 1.6s for up to 4m distance, considering the maximum EIRP

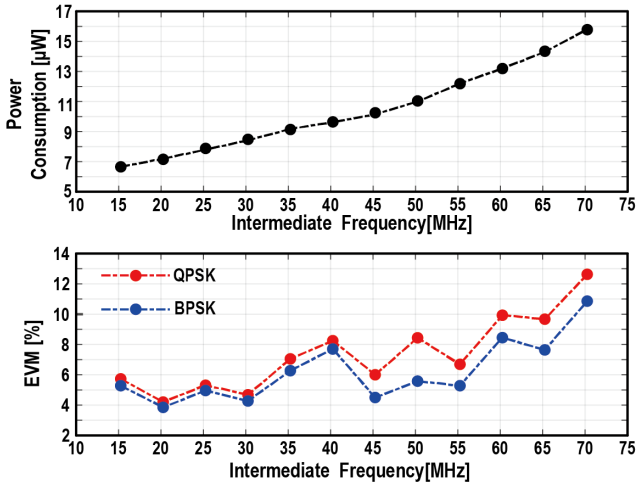


Fig. 9. Measured power consumption and EVM performance against IF frequencies.

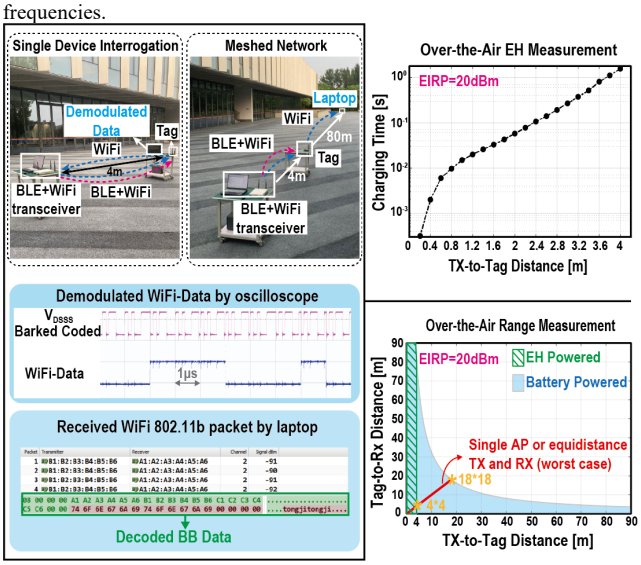


Fig. 10. Wireless testing setup; demodulated downlink WiFi BB data and decoded uplink WiFi packet with commodity TRX; over-the-air energy harvesting and range measurements.

of 20dBm for commodity BLE TXs. The proposed battery-less system achieves a TX-to-Tag-to-RX range of 8m (limited by EH) for single-AP networks, and that extends to 84m in a mesh network where an additional AP is available. In applications where a battery is an option, the proposed backscatter improves the worst-case distance (single AP or equidistance TX and RX) to 36m. For demodulation, the downlink data in both AP-to-Tag and Tag-to-Tag cases is successfully demodulated wirelessly into the BB, measured by the oscilloscope. Table I benchmarks the proposed backscatter system to prior WiFi backscatter systems. A die micrograph and the energy efficiency comparison to prior-arts are shown in Fig. 11.

## IV. Conclusion

This paper presents a low-power backscatter IC that supports peer-to-peer and fully 802.11b-WiFi-compatible bidirectional communication with state-of-the-art energy efficiencies for both uplink and downlink. This is achieved by implementing the proposed passive heterodyne RX and the reconfigurable pulse-shaped backscatter transmitter. The proposed chip supports frequency translation from all three BLE advertisement channels to every 802.11b channel (64

TABLE I COMPARISON TO STATE-OF-THE-ART

| | | VLSI'21 [4] | ISSCC'22 [3] | ISSCC'23 [6] | ISSCC'24 [7] | JSSC'24 [5] | This Work |
|---|---|---|---|---|---|---|---|
| Technology [nm] | | 180 | 65 | 65 | 65 | 180 | **65** |
| Core Area [mm²] | | 1.62 | 0.42 | 0.43 | 0.95 | 1.1 | **0.33** |
| Frequency [GHz] | | 2.4 | 2.4 | 2.4 | 2.4 | 2.4 | **2.4** |
| Power Scheme | | Solar | Battery | WPT: LTE | WPT: WiFi | WPT: Tone | **WPT: BLE** |
| Downlink RX | Scheme | WuRX | WuRX | WuRX | WiFi | - | **WiFi** |
| | Demodulation | Energy Detection-OOK | Energy Detection-OOK | Energy Detection-OOK | 802.11b-DBPSK | - | **802.11b-DBPSK** |
| | Date Rate | <62.5Kbps | <62.5Kbps | <62.5Kbps | 1Mbps | - | **1Mbps** |
| | Range | - | >30m | 50cm | - | - | **4m** |
| | RX Power [μW] | 0.15 | 4.5 | 4.5 | 3.5 | - | **4.3** |
| Uplink TX | Scheme | Tone to WiFi | WiFi-WiFi BLE-BLE | BLE to WiFi | WiFi to BLE | Tone to WiFi | **BLE to WiFi** |
| | Modulation | DBPSK | DBPSK/FSK | DB/QPSK | GFSK | DBPSK | **DB/QPSK** |
| | Date Rate | 1Mbps | 2Mbps | 2Mbps | 1Mbps | 1Mbps | **2Mbps** |
| | Pulse Shaping | No | No | No | No | No | **Yes** |
| | Equidistance TX and RX | Battery-less: 8m | Battery powered:17.5m | Battery-less: 50cm* | - | Battery-less: 4.5m (RX)-9m (TX) | **Battery-less: 4m* Battery powered:18m** |
| | EVM [%] | 24.74@ BPSK | - | - | - | 8.64@ BPSK | **3.85~10.86@BPSK** 4.2~12.63@QPSK**** |
| | TX Power [μW] | 2.5 | 39 | 11~45** | 17 | 0.87 | **6.6~15.8**** |
| Compatible to All WIFI Channels | | No (1 case) | No (2 cases) | No (8 cases) | No (1 case) | No (1 case) | **Yes (64 cases)** |
| **Peer-to-Peer Communication** | | No | No | No | No | No | **Yes** |

*Limited by energy harvester **Varies with IF

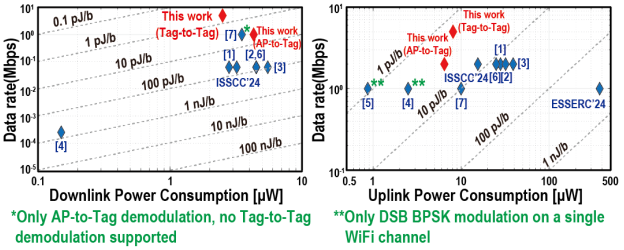


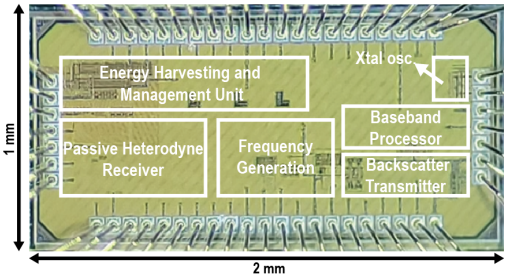


Fig. 11. Die micrograph and the energy efficiency comparison to prior WiFi backscatter systems.

cases) at low power. When implemented in commercial WiFi infrastructure, it achieves the single-antenna range of 36m with improved area efficiency.

## References


[1] P.-H. Wang et al., "A 28μW IoT Tag that can Communicate with Commodity WiFi Transceivers via a Single-Side-Band QPSK Backscatter Communication Technique," *ISSCC*, Feb. 2020.

[2] M. Meng et al., "Improving the Range of WiFi Backscatter Via a Passive Retro Reflective Single-Side-Band-Modulating MIMO Array and Non-Absorbing Termination," *ISSCC*, Feb. 2021.

[3] S. -K. Kuo et al., "A WiFi and Bluetooth Backscattering Combo Chip Featuring Beam Steering via a Fully-Reflective Phased-Controlled Multi-Antenna Termination Technique Enabling Operation Over 56 Meters," *ISSCC*, Feb. 2022.

[4] L. Lin et al., "Battery-Less IoT Sensor Node with PLL-Less WiFi Backscattering Communications in a 2.5-μW Peak Power Envelope," *VLSI Symp.*, 2021.

[5] M. Privitera et al., "Sub- μ W Battery-Less and Oscillator-Less Wi-Fi Backscattering Transmitter Reusing RF Signal for Harvesting, Communications, and Motion Detection," *JSSC*, 2024.

[6] S. -K. Kuo et al., "An LTE-Harvesting BLE-to-WiFi Backscattering Chip for Single-Device RFID-Like Interrogation," *ISSCC*, Feb. 2023.

[7] Z. Chang et al., "A Passive Crystal-Less Wi-Fi-to-BLE Tag Demonstrating Battery-Free FDD Communication with Smartphones," *ISSCC*, Feb. 2024.

[8] G. Papotto et al., "A 90-nm CMOS Threshold-Compensated RF Energy Harvester," *JSSC*, vol. 46, no.9, pp. 1985-1997, 2011.

[9] Z. Chang et al., "A Passive Bidirectional BLE Tag Demonstrating Battery-Free Communication in Tablet/Smartphone-to-Tag, Tag-to-Tablet/Smartphone, and Tag-to-Tag Modes," *ISSCC*, Feb. 2023.